IEEJ TRANSACTIONS ON ELECTRICAL AND ELECTRONIC ENGINEERING
IEEJ Trans 2016; **11**: 480–487
Published online in Wiley Online Library (wileyonlinelibrary.com). DOI:10.1002/tee.22265

Paper

2D-DOA Estimation Performance Using Split Vertical Linear and Circular Arrays

Karima Aouina[a], Non-member
Djamel Benazzouz, Non-member

This paper presents a new approach to reduce the computational complexity in two-dimensional (2D) matrix pencil (MP) method for direction of arrival (DOA) estimation of plane wave signals using a combination of vertical uniform linear array (VULA) and uniform circular array (UCA). By applying phase mode excitation based beamforming to the UCA, we can apply the matrix pencil (MP) method to the beamspace data using only a single snapshot. The technique is based on the split array, which is composed of two perpendicular arrays. The vertical uniform linear array used to determine the elevation DOA components is located perpendicularly at the center of the uniform circular array in the horizontal plane used to calculate the azimuth angles. Unlike common planar and circular arrays, this antenna array with its particular geometry requires no pair-matching between the azimuth and the elevation angle estimation and can also remove the drawbacks of estimation failure problems. Using this particular geometry for the 2D MP method leads to an efficient computational methodology for real-time implementation on a digital signal processor. The obtained simulation results of the MP method applied to both uncorrelated and correlated narrow-band sources in the presence of white noise show good performance estimation. © 2016 Institute of Electrical Engineers of Japan. Published by John Wiley & Sons, Inc.

Keywords: matrix pencil method, two-dimensional direction of arrival estimation, vertical uniform linear array, uniform circular array

Received 26 January 2015; Accepted 8 July 2015

1. Introduction

There have been many studies on the two-dimensional (2D) direction of arrival angle (DOA) estimation (azimuth and elevation angles) for incident signals on antenna element arrays [1–6]. It is an important issue in many applications, including radar, wireless communication, radio astronomy, seismic exploration, sonar, and electronic surveillance.

A planar array is required to estimate the source azimuth and elevation (2D angle estimation). Well-known planar arrays include two orthogonal uniform linear arrays, L shaped array[7], uniform rectangular array (URA)[6], and a uniform circular array (UCA)[8]. The UCA is able to provide 360° azimuthal coverage and a certain degree of source elevation information (depending on its element beam pattern). Note that the URA with non-omnidirectional elements is not able to provide full azimuthal coverage due to the directional beam pattern of its elements. In a beam-forming application, the directional patterns of a UCA can be electronically rotated throughout the azimuth without significant change in the beam shape. All elements on the UCA will exhibit identical beam pattern since the UCA has no edge elements and is less sensitive to the mutual coupling effects (compared to ULA and URA).

There exist many algorithms to estimate the 2D-DOA of signals received by the antenna arrays. Fernandez[7] proposed the matrix pencil (MP) method to estimate the 2D-DOA directly from the antenna employing an L-shaped array. Tayem and Kwon[9] proposed two 2D azimuth and elevation angle estimation algorithms, called *one* L-shape and *two* L-shape algorithms. They were applied using the propagator method. In[10], Harabi proposed a method based on the extended correlation matrix with two L-shaped antenna array configuration for 2D azimuth and elevation angle estimation problem. This method does not require any pair-matching for the 2D DOA estimation problems.

In Ref. [11], the authors proposed a 2D beam space matrix pencil (2D-BMP) method for DOA estimation of plane wave signals using a uniform rectangular array (URA). They used discrete Fourier transform to convert the complex signal subspace into a real and reduced dimensional beam space. In[12], a unitary transform for the 2D-MP method was formulated and used to transform the complex data matrix to a real matrix in order to reduce the computational complexity in DOA estimation problem using URA. Adiba [13] construct an enhanced matrix from the data samples. Then they use the MP method to extract the azimuth and elevation angles of arrival.

In Ref. [14], a hybrid algorithm was presented that combines the UCA-rank reduction (UCA-RARE) and Root-MUSIC algorithm for 2D direction-of-arrival (DOA) estimation of azimuth and elevation angle for UCAs in the presence of mutual coupling. The UCA-RARE algorithm was applied to estimate the azimuth angle independently of the elevation angle. Next, for each azimuth angle they performed a new search-free rooting algorithm based on the expansion of the array manifold into a double Fourier series.

In Ref. [15], a rigorous comparison between the 2D MUSIC and the 2D MP method is presented. The authors conclude that for the multiple 2D sinusoid case (and a one-measurement data model), the MP method is computationally much more efficient than MUSIC. In the context of a real-time implementation, it is highly desirable to develop methods that not only give good (DOA) estimation results but also require significantly reduced computational burden.

Recently, Albagory *et al*. [16] proposed an array structure for fast and computationally efficient 2D-DOA estimation using the MUSIC algorithm. This technique separates the noise and the signal subspace based on eigenvalue decomposition of the spatial covariance matrix. The conventional signal processing algorithms

[a] Correspondence to: Karima Aouina. E-mail: dbenazzouz@yahoo.fr

Solid Mechanics and Systems Laboratory (LMSS), University M'Hamed Bougara Boumerdes, Boumerdes 35000, Algeria

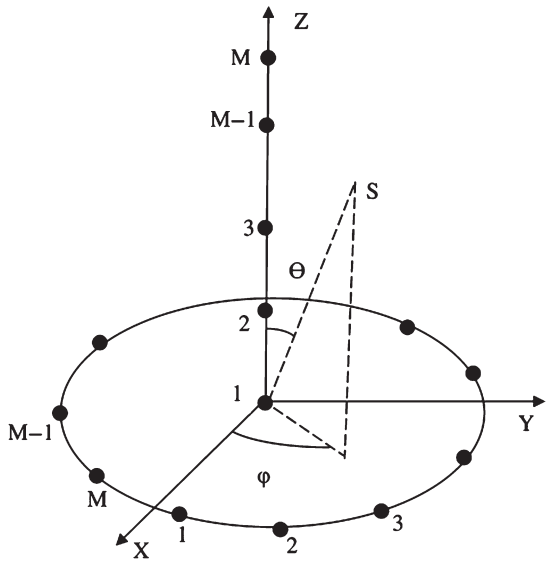

Fig. 1. Split array structure

using the covariance matrix works on the assumption that the signals impinging on the array are not coherent. Unlike the MUSIC algorithm, the MP method is known to work in an environment with correlated sources. This is due to the fact that the MP method works directly with data instead of the spatial covariance matrix; consequently, the nonstationary environment can be handled easily. Additionally, in Ref. [17] the author suggested that the MP method might outperform the more popular covariance methods when small numbers of data snapshots are utilized.

Our approach consists of applying the MP method to the split vertical linear and circular array. This array is composed of two subarrays, VULA which is used to determine the elevation DOA components, and UCA, which is used to determine the azimuth DOA components. Unlike in Ref. [16], we can work in an environment with correlated sources to estimate the DOA. On the other hand, the computational burden decreases several times than with the 2D-MP method proposed in Ref. [12,13] . The rest of the paper is organized as follows: The system model for the 2D-DOA with two perpendicular subarrays is presented in Section 2. The MP methods for the ULA and in UCA Beamspace are developed in Section 3. The performance of the 2D MP method using a Split array is presented in Section 4 and 5, followed by a conclusion.

2. System model

The antenna shape is presented in Fig. 1. The geometry of the array is composed of two perpendicular subarrays. The first is a ULA vertical subarray of M omnidirectional antenna elements and lies on the Z-axis. The second is a UCA horizontal subarray of M omnidirectional, identical, and uniformly distributed elements over the circumference of a circle with radius r in the XY plane.

Let us consider K narrow-band plane signals with wavelength λ_0 arriving at this array with an azimuth and an elevation angles (ϕi, θi). The signal vector $X(t)$impinging on the VULA array is defined as follows:

$$X_l(t) = xx(t) + N(t) \tag{1}$$

where

$$xx(t) = A_l(\theta)S(t) \tag{2}$$

$A_l(\theta) = [a_l(\theta_1), a_l(\theta_2), \ldots, a_l(\theta_K)]$ is a matrix that consists of the steering vectors of the linear array. $S(t) = [s_1(t), s_2(t), \ldots, s_K(t)]^T$ is the signal vector that consists of Kdifferent source signals. $N(t) = [N_0(t), N_1(t), \ldots, N_{M-1}(t)]^T$ is the white noise vector generated at each array element with zero mean and variance σ^2. The response steering vector of the VULA to a plane wave propagating from source $s_k(t)$ in the direction θ_k is defined as follows:

$$a_l(\theta_k) = [z_k^0 z_k^1 \cdots z_k^{M-1}] \tag{3}$$

where

$$z_k = e^{j\frac{2\pi}{\lambda_0}d\sin(\theta_k)} \tag{4}$$

Let us consider the center of the circle as the origin for the circular array. The circumferential spacing of adjacent elements in the array can be expressed by (5) and the antenna angular position by (6).

$$\mu = \frac{2\pi r}{M} \tag{5}$$

$$\gamma_i = \mu i = \frac{2\pi r}{M} i, i = 0, 1, \ldots, M-1 \tag{6}$$

So, we can describe the phase delay seen at antenna element i relative to the center of the array for the plane wave approaching signal from the azimuth direction by (7). Similarly for the VULA, the signal vector received by the array will be given by (8).

$$\Psi_i = \frac{2\pi}{\lambda} r\cos(\varphi - \gamma_i) \tag{7}$$

$$X_c(t) = A_c(\theta, \varphi)S(t) + N(t) \tag{8}$$

where $A_c(\theta, \varphi) = [a_l(\theta_1, \varphi_1), a_l(\theta_2, \varphi_2), \ldots, a_l(\theta_K, \varphi_K)]$ is the matrix consisting of the steering vectors of the circular array. The element-space steering vector of the UCA is defined by (9):

$$a_c(\theta, \varphi) = \begin{bmatrix} e^{j\frac{2\pi}{\lambda}r\sin(\theta)} & e^{j\frac{2\pi}{\lambda}r\sin(\theta)} & \cdots & e^{j\frac{2\pi}{\lambda}r\sin(\theta)} \\ \cos(\varphi) & \cos(\varphi - \gamma_1) & & \cos(\varphi - \gamma_{M-1}) \end{bmatrix} \tag{9}$$

3. Matrix Pencil Method

3.1. MP method for ULA As presented in Ref. [18], the MP method for DOA estimation begins with the waveforms received by the ULA in the form given by (1). This equation can be sampled with periodT_s at discrete time instants nT_s, and the discrete time sampled version $X_l(nT_s)$ is represented simply by $X_l(n)$. The linear beam former output can be written as $YY_l(n) = W_l^T X_l(n)$, where W_l^T represents the weights transpose matrix.

$$X_l(n) = xx(n) + N(n) \tag{10}$$

In summation notation

$$x_i(n) = \sum_{k=1}^{K} s_k(n) z_k^i + N_i(n) \tag{11}$$

Let us build the Hankel matrix $Y$from the original data vector $\{xx(0)xx(1)\ldots xx(M-1)\}$.

$$Y = \begin{bmatrix} xx(0) & xx(1) & \cdots & xx(L-1) \\ xx(1) & xx(2) & \cdots & xx(L) \\ \vdots & \vdots & \ddots & \vdots \\ xx(M-L) & xx(M-L+1) & \cdots & xx(M-1) \end{bmatrix}$$
$$(M-L+1) \times (L) \tag{12}$$

The parameter L is called the pencil parameter. In previous works [19], it has been shown that in the interest of efficient noise filtering, it is best to choose L between the values $\frac{M}{3}$ and $\frac{M}{2}$.

The next step is to define two submatrices of Y, denoted as Y_a and Y_b. We will generate these matrices by deleting a single row of Y for each submatrix. Let us delete the last row of Y to form Y_a and the first row of Y to form Y_b. This yields the matrices Y_a and Y_b.

$$Y_a = \begin{bmatrix} xx(0) & xx(1) & \dots & xx(L-1) \\ xx(1) & xx(2) & \dots & xx(L) \\ \vdots & \vdots & \ddots & \vdots \\ xx(M-L-1) & xx(M-L) & \dots & xx(M-2) \end{bmatrix} \quad (M-L)\times(L) \tag{13}$$

$$Y_b = \begin{bmatrix} xx(1) & xx(2) & \dots & xx(L) \\ xx(2) & xx(3) & \dots & xx(L+1) \\ \vdots & \vdots & \ddots & \vdots \\ xx(M-L) & xx(M-L+1) & \dots & xx(M-1) \end{bmatrix} \quad (M-L)\times(L) \tag{14}$$

One can write

$$Y_a = Z_a X_0 Z_b \tag{15}$$

$$Y_b = Z_a X_0 Z_0 Z_b \tag{16}$$

where the matrices Z_a, Z_b, X_0, and Z_0 are defined as follows:

$$Z_a = \begin{bmatrix} 1 & 1 & \dots & 1 \\ z_1 & z_2 & \dots & z_K \\ \vdots & \vdots & \ddots & \vdots \\ z_1^{M-L-1} & z_2^{M-L-1} & \dots & z_K^{M-L-1} \end{bmatrix} \quad (M-L)\times(K) \tag{17}$$

$$Z_b = \begin{bmatrix} 1 & z_1 & \dots & z_1^{L-1} \\ 1 & z_2 & \dots & z_2^{L-1} \\ \vdots & \vdots & \ddots & \vdots \\ 1 & z_K & \dots & z_K^{L-1} \end{bmatrix} (K)\times(L) \tag{18}$$

$$X_0 = diag\{s_1, s_2, \dots, s_K\} \tag{19}$$

$$Z_0 = diag\{z_1, z_2, \dots, z_K\} \tag{20}$$

Thus, we can express the MP to extract the DOA information as follows:

$$Y_b - \lambda Y_a = Z_a X_0 Z_0 Z_b - \lambda Z_a X_0 Z_b \tag{21}$$

Rewriting (21) in another form, we get

$$Y_b - \lambda Y_a = Z_a X_0 (Z_0 - \lambda I) Z_b \tag{22}$$

where I represents the $K \times K$ identity matrix. It has been shown [19] that, in general, the rank of $Y_b - \lambda Y_a$ is K provided $K \le L \le M - K$.

From (22), we can easily see on the right side that the rank-reducing values of the pencil are the values of λ that reduce the rank of the $Z_0 - \lambda I$ term, namely $\lambda = z_1, z_2, \dots z_K$. When λ is set to z_i, the ith row of the $Z_0 - \lambda I$ term becomes zero, and the rank of the pencil becomes $K - 1$. As stated in Ref. [18], the solutions of the pencil λ can thus be found as the generalized eigenvalues of the matrix pair$\{Y_a, Y_b\}$, or, equivalently, as the eigenvalues of $\{Y_a^+ Y_b - \lambda I\}$, where Y_a^+ is the Moore–Penrose pseudo-inverse of Y_a, defined by (23).

$$Y_a^+ = (Y_a^H Y_a)^{-1} Y_a^H \tag{23}$$

The superscript H denotes the conjugate transpose.

Concerning the noisy data, we form an approximation of the matrix Y from the components $x_i(n)$, $i = 0, 1, \dots, M-1$, of the observed signal vector $X_l(n)$.

$$\hat{Y} = \begin{bmatrix} x(0) & x(1) & \dots & x(L-1) \\ x(1) & x(2) & \dots & x(L) \\ \vdots & \vdots & \ddots & \vdots \\ x(M-L) & x(M-L+1) & \dots & x(M-1) \end{bmatrix} \quad (M-L+1)\times(L) \tag{24}$$

Singular value decomposition (SVD) is useful to reduce some of the noise effect. The matrix $\hat{Y}$ obtained by (24) can be written as

$$\hat{Y} = U \sum V^H \tag{25}$$

where U and V are unitary matrices with columns that are eigenvectors of $\hat{Y}\hat{Y}^H$ and $\hat{Y}^H\hat{Y}$, respectively, and $\sum$ is a diagonal matrix containing the singular values of $\hat{Y}$ in the decreasing order $\sigma_1 \ge \sigma_2 \ge \dots \ge \sigma_{\min}$. Generally, $\sum$ is not necessarily a square matrix. At this point, if the incident number of signals is unknown, the procedure suggested in[18] and described in Ref. [20] can be used to estimate K. This can be done by setting K to the largest i for which $10^{-r} \approx \sigma_i/\sigma_{\max}$, where r is the significant number of decimal digits in the data vector $X_l(n)$.

After computing the SVD of the data matrix $\hat{Y}$, the matrix is divided into two subspaces, identified as signal subspace and noise subspace. The matrices $\hat{Y}_a$ and $\hat{Y}_b$ are constructed from the signal subspace matrix.

DOAs are then extracted from the eigenvalues $z_i = \lambda_i$ as

$$\theta_i = \sin^{-1}\left(\frac{Im\{\ln(z_i)\}}{\frac{2\pi}{\lambda_0}d}\right) \tag{26}$$

3.2. MP method in UCA beamspace Phase mode excitation-based beam-forming is given in [21]. Some complementary comments were provided in [22]. Phase mode excitation-based beam-forming assigns a weight w_i to the output of the array element i, where all weights have equal magnitude. The phase of the weight w_i is assigned in a linear manner based on the angular position of the array element i relative to the reference element. Spatial harmonics of this excitation pattern are also of interest, where the linear relationship between angular distance of the element $i$and the assigned phase of w_i is increased by an integer multiple m. The beam-formed response of the array, generated by using the weights assigned based on the spatial harmonic m, is known as the response of the array due to the excitation of phase mode m.

We define the beam-forming weight vector that excites the array with phase mode m as follows:

$$w_m = \frac{1}{M}[1 e^{-j2\pi m/M} \dots e^{-j2\pi m(M-1)/M}]^T \tag{27}$$

By applying the beam-forming weights to the manifold of the circular array, the spatial response pattern of the UCA after beam-forming based on excitation of phase mode m can be approximated by (28).

$$f_m(\varphi) = w_m^H a_c(\theta, \varphi) \approx j^{|m|} J_{|m|}\left(\frac{2\pi}{\lambda_0} r \sin(\theta)\right) e^{jm\varphi} \tag{28}$$

where $J_i(x)$ is the Bessel function of the first kind of order i. Notice that the maximum number of modes is given by

$$D \approx \frac{2\pi}{\lambda_0} r \tag{29}$$

Selection of an appropriate value for the maximum excited mode D is discussed in detail in [21]. Collecting the weights for all

modes of interest $|m| \leq D$, we define the phase mode excitation beam-former as follows:

$$\tilde{F}_{pm}^{H} = CV^{H} \tag{30}$$

where

$$C = diag\{j^{-M}, \ldots, j^{-1}, j^{0}, j^{1}, \ldots, j^{M}\} \tag{31}$$

$$V^{H} = \sqrt{M}[w_{-D}| \cdots |w_0| \ldots |w_D] \tag{32}$$

By applying the beam-former to the UCA manifold, we can deduce the UCA beamspace manifold as

$$\tilde{a}(\varphi) = \tilde{F}_{pm}^{H} a_c(\theta, \varphi) = CV^{H} a_c(\theta, \varphi) = \sqrt{M} J_\zeta v(\theta, \varphi) \tag{33}$$

where

$$J_\zeta = diag\left\{J_{-D}\left(\frac{2\pi}{\lambda_0} r \sin(\theta)\right), \ldots, J_0\left(\frac{2\pi}{\lambda_0} r \sin(\theta)\right), \ldots, J_D\left(\frac{2\pi}{\lambda_0} r \sin(\theta)\right)\right\} \tag{34}$$

$$v(\varphi) = [e^{-jD\varphi}, \ldots, e^{-j\varphi}, e^{j0}, e^{j\varphi}, \cdots, e^{jD\varphi}]^{T} \tag{35}$$

The beamspace manifold $\tilde{a}(\varphi)$ exhibits the Vandermonde form through the vector$v(\varphi)$. The observed signal vector can be expressed in the beam space as

$$\tilde{y}(n) = \begin{bmatrix} \tilde{y}_{-D}(n) \\ \vdots \\ \tilde{y}_D(n) \end{bmatrix} = F_{pm}^{H} y_c(n) = \sum_{k=1}^{K} (\tilde{a}(\theta_k, \varphi_k) s_k(n)) + \tilde{N}(n) \tag{36}$$

For a single mode, the expression of the observed excitation can be expressed as

$$\tilde{y}_m(n) = \sum_{k=1}^{K} J_{|m|}\left(\frac{2\pi}{\lambda_0} r \sin(\theta)\right) e^{jm\varphi_k} s_k(n) + \tilde{N}_m(n) \tag{37}$$

for $-D \leq m \leq D$. Notice that the Bessel function term $J_{|m|}(\frac{2\pi}{\lambda_0} r \sin(\theta))$ is independent of k. By applying the normalization coefficient $\delta_m = \frac{1}{J_{|m|}\left(\frac{2\pi}{\lambda_0} r \sin(\theta)\right)}$ to each element of the beamspace data vector, we get

$$\bar{y}_m(n) = \delta_m \tilde{y}_m(n) = \frac{\tilde{y}_m(n)}{J_{|m|}\left(\frac{2\pi}{\lambda_0} r \sin(\theta)\right)} = \sum_{k=1}^{K} s_k(n) e^{jm\varphi_k} + \bar{N}_m(n) \tag{38}$$

Notice that (38) has the same form as (11). Similarly, following the same analysis for ULA, we can construct the normalized beamspace data matrix $\bar{Y}$ and the two submatrices $\bar{Y}_a$, $\bar{Y}_b$ as follows:

$$\bar{Y} = \begin{bmatrix} \bar{y}(-D) & \ldots & \bar{y}(-D + (L-1)) \\ \vdots & \ddots & \vdots \\ \bar{y}(D - (L-1)) & \ldots & \bar{y}(D) \end{bmatrix}_{(M' - L + 1) \times (L)} \tag{39}$$

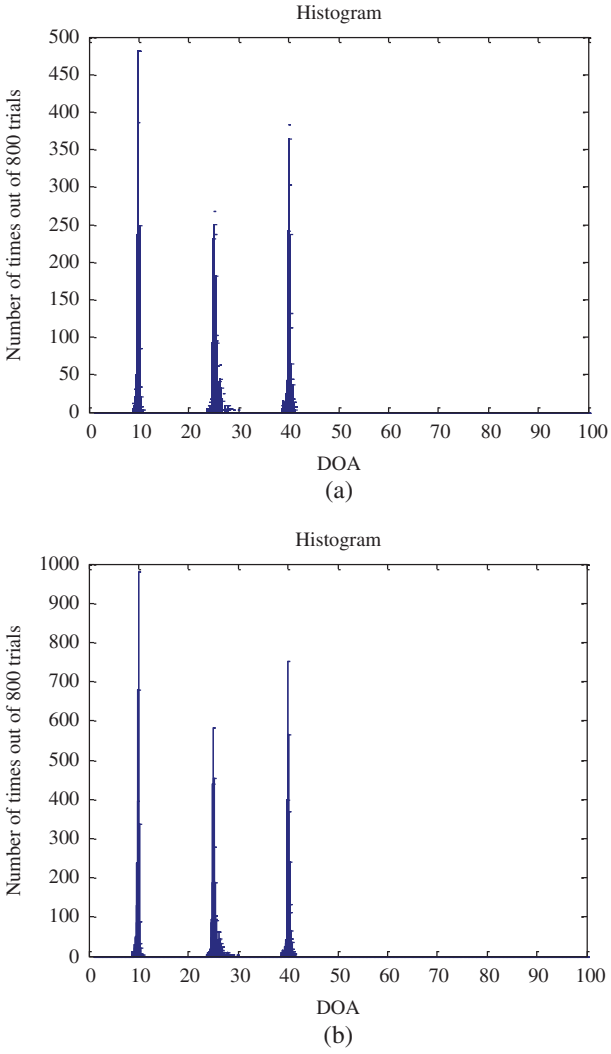

Fig. 2. Histogram of the elevation angles (10°, 25°, 40°) (a) Accuracy of MP for SNR = 5 dB and (b) Accuracy of MP for SNR = 10 dB

$$\bar{Y}_a = \begin{bmatrix} \bar{y}(-D) & \ldots & \bar{y}(-D + (L-1)) \\ \vdots & \ddots & \vdots \\ \bar{y}(D - (L-1) - 1) & \ldots & \bar{y}(D-1) \end{bmatrix}_{(M' - L) \times (L)} \tag{40}$$

$$\bar{Y}_b = \begin{bmatrix} \bar{y}(-D+1) & \ldots & \bar{y}(-D + (L-1) + 1) \\ \vdots & \ddots & \vdots \\ \bar{y}(D - (L-1)) & \ldots & \bar{y}(D) \end{bmatrix}_{(M' - L) \times (L)} \tag{41}$$

Table I. Comparison of computation complexity

	2D-EMP (URA)	2D-UMP (URA)	2D-MP (split array)
SVD	$4\frac{17}{3}(EL)^3 + 4(EL)^2KF$ multiplications	$\frac{17}{3}(KL)^3 + (KL)^2EF$ multiplications	$4\frac{17}{3}(M-L+1)^3 + 4(M-L+1)^2L + 4\frac{17}{3}(M'-L+1)^3 + 4(M'-L+1)^2L$ multiplications
Example of computations given in Section 5	3 333 300 multiplications	151 040 multiplications	37 552 multiplications

$E = M - K + 1$ and $F = N - L + 1$

where $M' = 2D + 1$. Thus we can write it in the form given by (42) and (43).

$$\bar{Y}_a = \bar{Z}_a X_0 \bar{Z}_b \tag{42}$$

$$\bar{Y}_b = \bar{Z}_a X_0 Z_0 \bar{Z}_b \tag{43}$$

$$\bar{Z}_a = \begin{bmatrix} zz_1^{-D+L'} & \cdots & zz_K^{-D+L'} \\ zz_1^{-D+L'+1} & \cdots & zz_K^{-D+L'+1} \\ \vdots & \vdots & \vdots \\ zz_1^{L'} & \cdots & zz_K^{L'} \\ \vdots & \vdots & \vdots \\ zz_1^{D-L'} & \cdots & zz_K^{D-L'} \end{bmatrix}$$

$$((2D+1) - L) \times (K) \tag{44}$$

$$\bar{Z}_b = \begin{bmatrix} zz_1^{-L'} & zz_1^{-L'+1} & \cdots & zz_1^{L'-1} \\ \vdots & \vdots & \vdots & \vdots \\ zz_K^{L'} & zz_K^{-L'+1} & \cdots & zz_K^{L'-1} \end{bmatrix} (K) \times (L) \tag{45}$$

$$X_0 = diag\{s_1, s_2, \ldots, s_K\} \tag{46}$$

$$Z_0 = diag\{zz_1, zz_2, \ldots, zz_K\} \tag{47}$$

where $zz_k = e^{j\varphi_k}$ and $L' = \frac{L}{2}$

With (42) and (43), we can apply the MP algorithm as described in Section 3.1.

4. Computational Complexity

In the 2D-MP method, the most computational load is to estimate the signal subspace, which requires an SVD of a data matrix and pairing computation. If we consider a 2D-URA with M and N sensors along the x- and y-directions, then K and L are the pencil parameters. In the 2D-EMP method [13], the data matrix is complex of size $L(M - K + 1) \times K(N - L + 1)$. In the 2D-UMP method[12], the data matrix is transformed into a real matrix of size $KL \times 2(M - K + 1)(N - L + 1)$. Note that one complex multiplication requires four real multiplications, therefore 2D-UMP requires 4 times less computations as compared to the 2D-MP method. Computing the SVD of 2D-UMP requires $\frac{17}{3}(KL)^3 + 2(KL)^2(M - K + 1)(N - L + 1)$ multiplications[12–23]. For 2D-EMP, it needs $4\frac{17}{3}((M - K + 1)L)^3 + 4((M - K + 1)L)^2 K(N - L + 1)$multiplications. However, in the split array configuration, our data matrix are complex of size $(M - L + 1) \times L$ for VULA and $(M' - L + 1) \times L$ for UCA. So computing the SVD of 2D-MP split array requires $4\frac{17}{3}((M - L + 1)^3 + (M' - L + 1)^3) + 4((M - L + 1)^2 L + (M' - L + 1)^2 L)$ multiplications[23].

The correct pairing used in [13] reduces the complexity of the computation compared to the one used in[12], which uses more operations like Kronecker product and additions. Unlike in [12,13], 2D-MP with a split array does not need a pairing algorithm that reduces the computational burden faced in 2D-UMP and 2D-EMP methods. Table I summarizes the SVD computation of the two methods compared to our approach.

5. Simulation Results

The MP method's performance using a split array is given in this section. The noise is assumed to be zero-mean white Gaussian noise of variance σ, and the complex amplitudes of signals are equal to 1. Assume three signals impinging on the split array having the following directions: (10°, 50°), (25°, 70°), and (40°, 120°). For the linear array, the distance between the antenna elements is $\frac{\lambda}{2}$, the pencil parameter is chosen to be $L = 5$, and

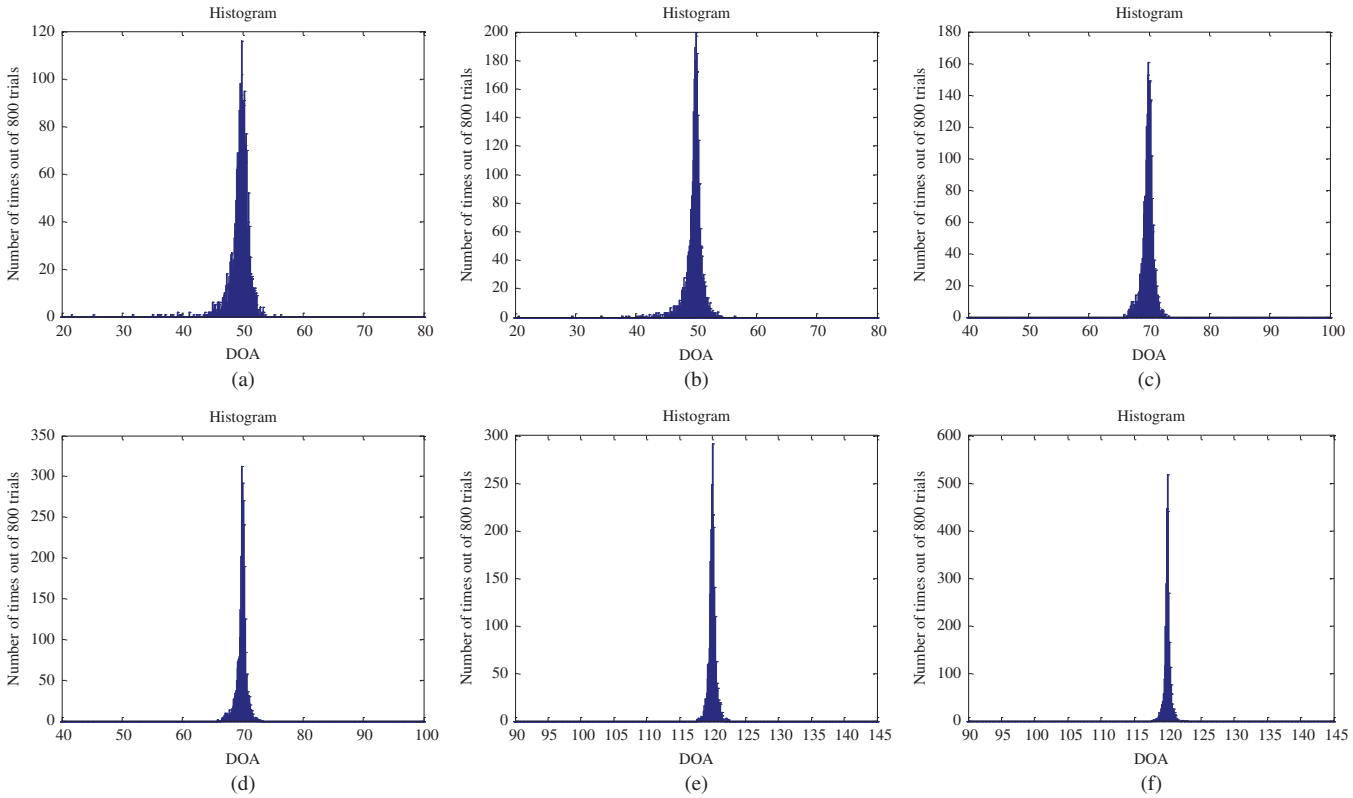

Fig. 3. Histogram of the azimuth angles (50°, 70°, 120°), (a, b) Accuracy of MP, for 50° (for SNR = 5 and 10 dB, respectively), (c, d) Accuracy of MP, for 70° (for SNR = 5 and 10 dB, respectively) and (e, f) Accuracy of MP, for 120° (for SNR = 5 and 10 dB, respectively)

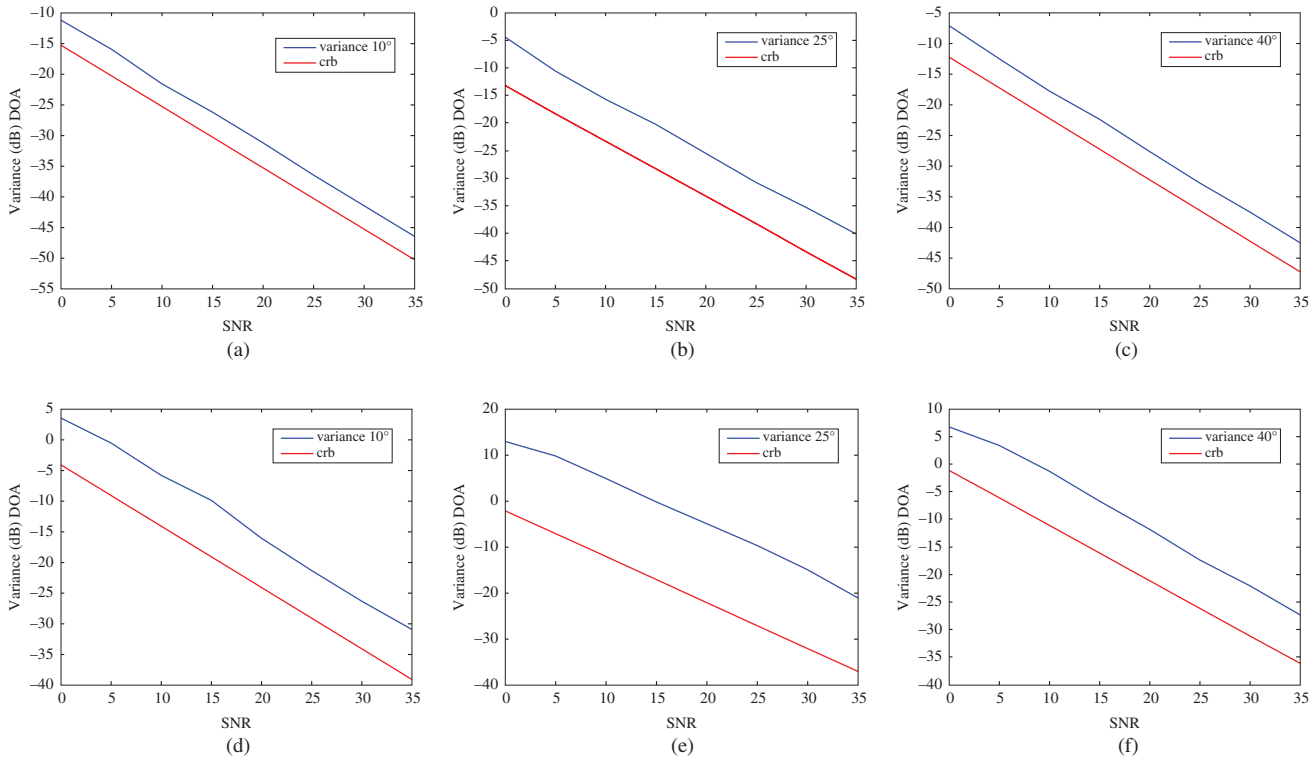

Fig. 4. Variance of MP for the elevation angles (10°,25°,40°) versus SNR: (a)–(c) for $M = 14$, $L = 6$; (d)–(f) for $M = 8$, $L = 3$

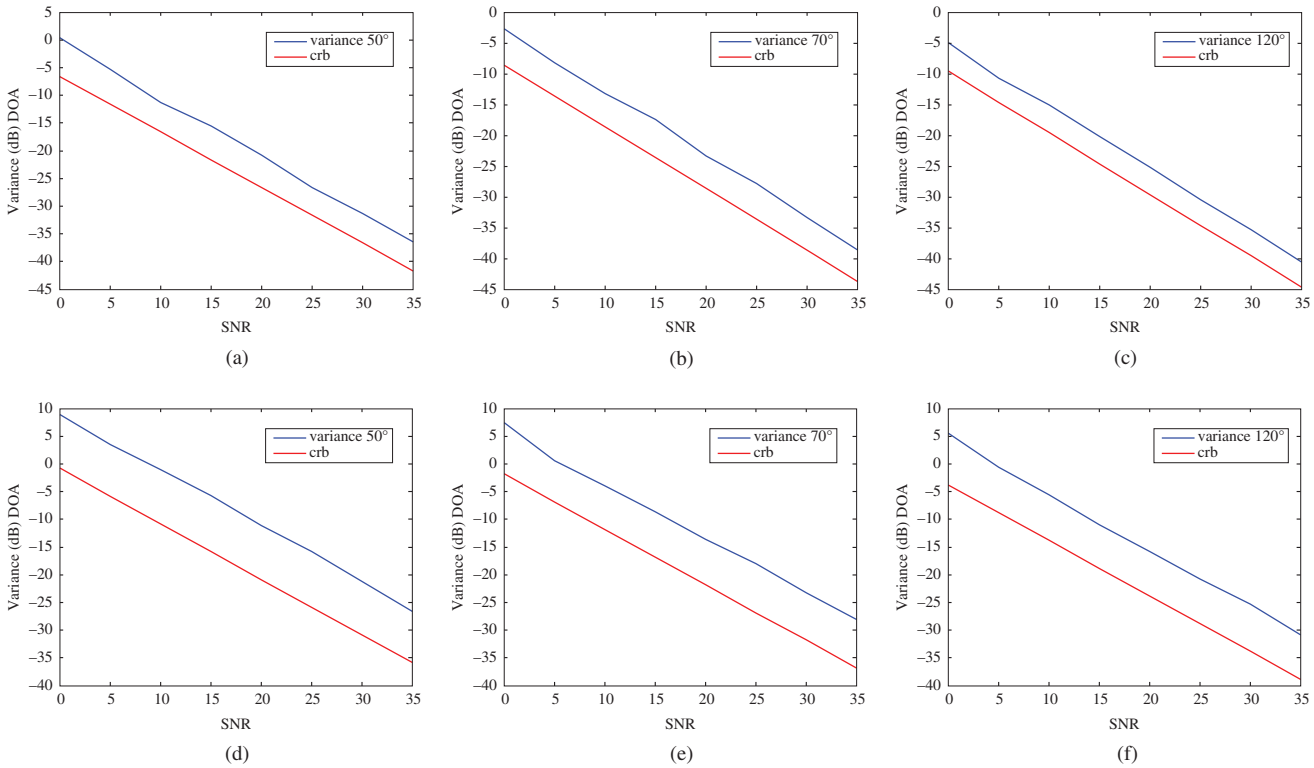

Fig. 5. Variance of MP for the azimuth angles (50°, 70°,120°) versus SNR: (a)–(c) for $M = 14$, $L = 6$; (d)–(f) for $M = 8$, $L = 3$

the number of data snapshots is 800. For the circular array, the UCA radius, the maximum mode, the total number of modes, and the pencil parameter are chosen to be, respectively, $0.949\lambda_0$, 6, 13, and 6. For this array only one snapshot is used. First we consider 14 antenna elements for each array. Figure 2 shows the histogram plots for the elevation angles, and Fig. 3 shows the histogram plots for each azimuth angles. Notice that in each case, the applied method gives close elevation and azimuth DOA estimation. The clear peaks appear around (10°, 25°, 40°) for elevation angles and (50°, 70°, 120°) for azimuth angles. Notice that we determine the azimuth angles separately for each identified elevation angle and apply the parallel processing to reduce the time of calculations. The histogram plot is given for 800 trials.

Figures 4 and 5 show the sample variance of the elevation angle estimations versus the signal-to-noise ratio (SNR) and the sample variance of the azimuth angle estimations versus the SNR,

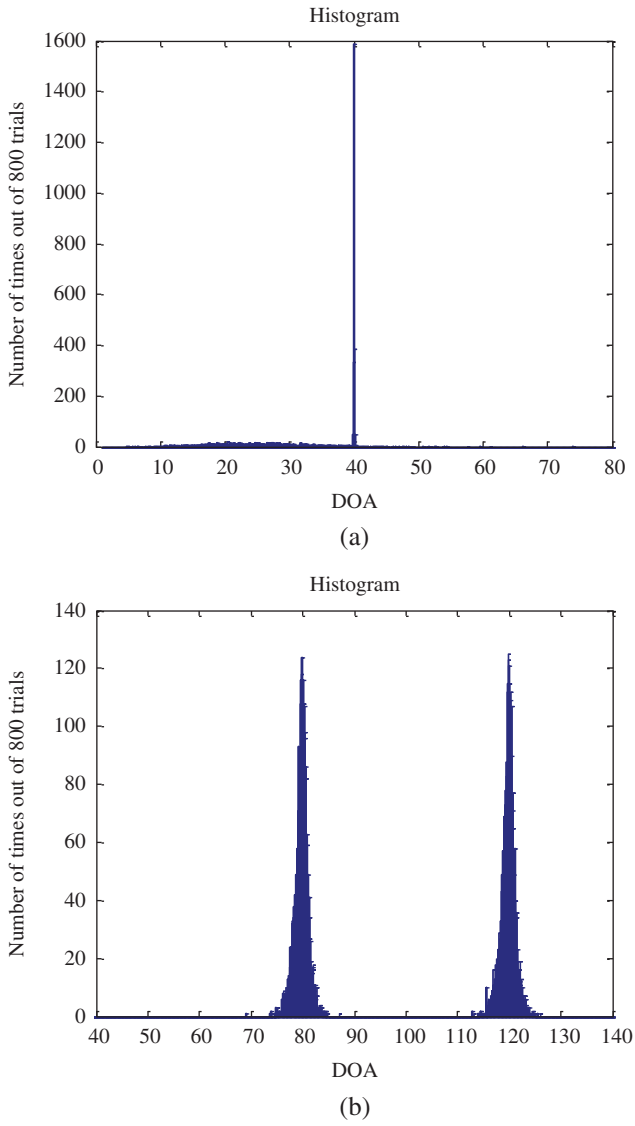

Fig. 6. Histogram of two coherent co-elevation sources located at (40°,80°) and (40°,120°), SNR = 10 dB. (a) Histogram of the elevation angles (40°, 40°) and (b) for azimuth angles (80°,120°)

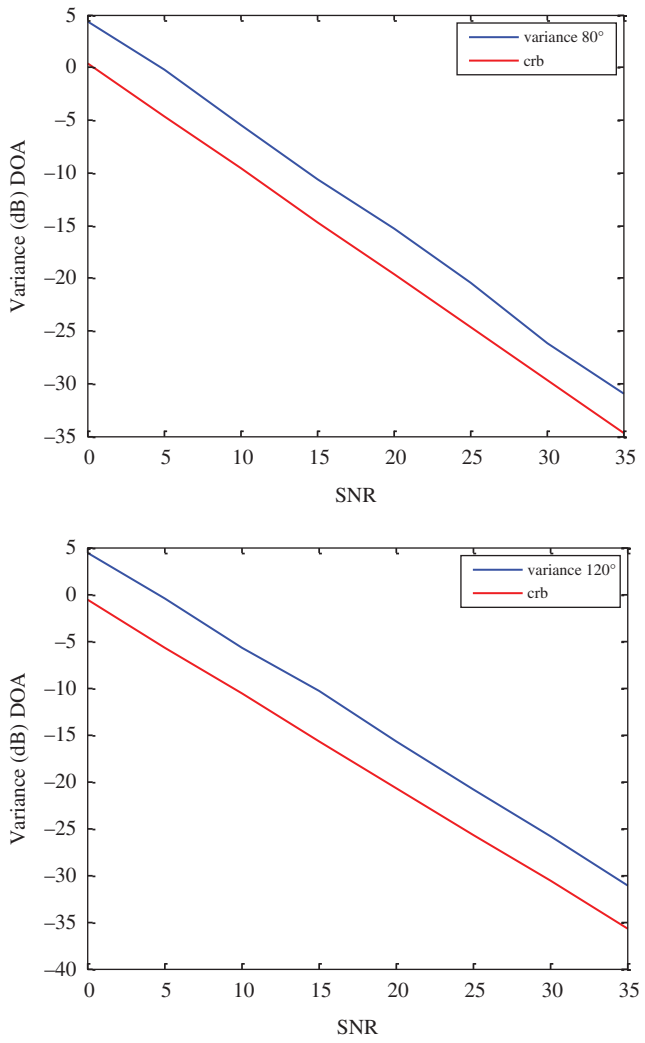

Fig. 7. Variance of MP for the azimuth angles (80°, 120°) versus SNR

respectively. We note that 2D-MP with this array gives better performance when the number of sensors increases. Notice that under poor conditions (low SNR), the array provides good result. The Cramer–Rao lower bound (CRB) is also calculated and shown in Figs. 4 and 5.

Considering the scenario of two coherent sources with the same elevation angle coming from (40°, 80°) and (40°, 120°), the attenuation coefficient is $0.9\exp(j\pi/4)$. For the linear array, the pencil parameter is chosen to be $L = 5$ and the number of data snapshots is 100. The histogram plots for each elevation and azimuth angle are shown in Fig. 6. We notice that there is a single peak for the elevation angles and there are two peaks for the azimuth angles.

Figure 7 presents the sample variance of the azimuth angle estimations versus the SNR. The CRB is also calculated and shown in Fig. 7. We observe that the MP method has less resolution in presence of coherent sources than for uncorrelated sources.

6. Conclusion

In this study, the MP 2D-DOA method was used with a split array. This array was composed of two perpendicular arrays: the vertical linear array and the circular array in the horizontal plane. The first was used to determine the elevation DOA component, and afterward the second allowed us to calculate the azimuth angles separately. This represents a configuration that does not require any matching pair for the 2D-DOA estimation problems. The obtained results show clearly that the technique can detect co-elevation coherent sources that have different azimuth angles. The proposed model gives good performance at low SNR and for close sources. Also, the MP method retains the ability to detect coherent signals. The MP method in UCA beamspace can estimate the azimuth angles using only one snapshot. Hence, the computational complexity can be further reduced, which allows real-time implementation on a digital signal processor.

References

(1) Wu Y, Liao G, So HC. A fast algorithm for 2-D direction-of-arrival estimation. *Signal Processing* 2003; **83**:1827–1831.
(2) Xie J, He Z, Li H, Li J. 2D DOA estimation with sparse uniform circular arrays in the presence of mutual coupling. *EURASIP Journal on Advances in Signal Processing* 2011; **2011**:127.
(3) Li P, Yu B, Sun J. A new method for two-dimensional array signal processing in unknown noise environments. *Signal Processing* 1995; **47**:319–327.
(4) Wu Y, So HC. Simple and accurate two-dimensional angle estimation for a single source with uniform circular array. *IEEE Antennas and Wireless Propagation Letters* 2008; **7**:78–80.

(5) Yilmazer N, Sarkar TK. Efficient computation of the azimuth and elevation angles of the sources by using unitary matrix pencil method (2-D UMP). *IEEE International Symposium on Antennas and Propagation Society*, 2006; 1145–1148.
(6) Zoltowski MD, Haardt M, Mathews CP. Closed-form 2-D angle estimation with rectangular arrays in element space or beamspace via unitary ESPRIT. *IEEE Transactions on Signal Processing* 1996; **44**:316–328.
(7) Fernandez del Rio JE, Catedra-Perez MF. The matrix pencil method for two dimensional direction of arrival estimation employing an L-shaped array. *IEEE Transactions on Antennas and Propagation* 1997; **45**(**11**):1693–1694.
(8) Tan CM, Fletcher P, Beach MA, Nix AR, Landmann M, Thomä RS. On the Application of Circular Arrays in Direction Finding Part I: Investigation into the estimation algorithms. *1st Annual COST 273 Workshop*, Espoo, Finland, 2002; 29–30.
(9) Tayem N, Kwon HM. L-shape 2-dimensional arrival angle estimation with propagator method. *IEEE Transactions on Antennas and Propagation* 2005; **53**(**11**):1622–1630.
(10) Harabi F, Changuel H, Gharsallah A. Estimation of 2-D direction of arrival with an extended correlation matrix. *IAENG International Journal of Computer Science* 2007; **33**(**11**):25.
(11) Khan MF, Tufail M. Computationally efficient 2D beamspace matrix pencil method for direction of arrival estimation. *Digital Signal Processing* 2010; **20**:1526–1534.
(12) Yilmazer N, Sarkar TK. 2-D unitary matrix pencil method for efficient direction of arrival estimation. *Digital Signal Processing* 2006; **16**:767–781.
(13) Adiba EF, Bri S, Habibi M, Medouri A. Application of 2-D enhanced matrix pencil method for efficient direction of arrival. *International Journal of Science and Advanced Technology* 2011; **1**(**6**):31–36.
(14) Goossens R, Rogier H. A hybrid UCA-RARE/Root-MUSIC approach for 2-D direction of arrival estimation in uniform circular arrays in the presence of mutual coupling. *IEEE Transactions on Antennas and Propagation* 2007; **55**(**3**):841–849.
(15) Yang H, Hua Y. Asymptotic properties of 2-D MUSIC estimator and comparison to 2-D MP estimator. *Signal Processing* 1994; **40**:257–268.
(16) Albagory Y, Ashour A. MUSIC 2D-DOA estimation using split vertical linear and circular arrays. *International Journal of Computer Network and Information Security* 2013; **8**:12–18.
(17) Yilmazer N, Ari S, Sarkar TK. Multiple snapshot direct data domain approach and ESPRIT method for direction of arrival estimation. *Digital Signal Processing* 2008; **18**:561–567.
(18) Yilmazer N, Jinhwan K, Sarkar TK. Utilization of a unitary transform for efficient computation in the matrix pencil method to find the direction of arrival. *IEEE Transactions on Antennas and Propagation* 2006; **54**(**1**):175–181.
(19) Hua Y, Sarkar TK. Matrix pencil method for estimating parameters of exponentially damped/undamped sinusoids in noise. *IEEE Transactions on Acoustics, Speech and Signal Processing* 1990; **38**(**5**):814–824.
(20) Sarkar TK, Pereira O. Using the matrix pencil method to estimate the parameters of a sum of complex exponentials. *Transactions on Antennas and Propagation* 1995; **37**(**1**):48–55.
(21) Mathews CP, Zoltowski MD. Eigenstructure techniques for 2-D angle estimation with uniform circular arrays. *IEEE Transactions on Signal Processing* 1994; **42**(**9**):2395–2407.
(22) Mathews CP, Zoltowski MD. Signal subspace techniques for source localization with circular sensor arrays. *ECE Technical Reports Paper* 172, Purdue e-Pubs, 1994.
(23) Golub GH, Van Loan CF, *Matrix Computations*, 3rd ed. Johns Hopkins University Press: Baltimore, MD; 1996

Karima Aouina Aliouche (Non-member) was born in 1968 in Constantine, Algeria. She received the Engineer and Magister degrees in electronics from the University of Constantine, Algeria, in 1992 and 1997, respectively. She is currently working toward the Ph.D. degree in signal processing at the Solid Mechanics and Systems Laboratory (LMSS), University M'Hamed Bougara Boumerdes, Algeria. Her current research interests include digital signal processing, mobile communications, and adaptive antenna problems.

D. Benazzouz (Non-member) obtained the Magister and Engineering degree in applied electronics from the INELEC Institute in 1991and 1982, respectively, and the Doctorat d'Etat degree in electronics from ENP–Algiers in 1999. His doctoral work was on the performance evaluation of parallel distributed systems. Between 1982 and 1983, he was an engineer with the Algerian petroleum company SONTRACH. Between 1983 and 1985, he was an engineer with the Algerian electrical company SONELGAZ. Since 1986, he has been a Senior Professor with the Department of Industrial Maintenance, University M'Hamed Bougara Boumerdes, Algeria. He joined the Solid Mechanics and Systems Laboratory (LMSS) in 2000. His interests include Petri nets contribution in complex systems, fault detection and isolation, electromechanical system fault detection and diagnosis, risk assessment and dynamic reliability systems.